The Monomode Fiber—A New Tool for Holographic Interferometry

Monomode and multimode fibers with step-index profiles are used as tools to measure surface displacement by holographic interferometry

by J.A. Gilbert, T.D. Dudderar, M.E. Schultz and A.J. Boehnlein

ABSTRACT—Monomode fibers are used to minimize modal interactions which ordinarily occur during holographic deformation studies based on multimode fiber-optic access. Test results show that holograms have better diffraction efficiency than those generated using multimode fibers and that stringent requirements for vibration isolation associated with holographic testing can be somewhat relaxed.

List of Symbols

a = radius of plate
a_j = modal amplitude
d = displacement vector
d_i = inner diameter of pipe
d_o = outer diameter of pipe
$\hat{e}_i$ = unit vector in the direction of propagation
e_j = modal field
h = thickness of plate
n = fringe-order number
n_{cl} = index of refraction of cladding
n_{co} = index of refraction of core
r, θ, Z = cylindrical coordinates
x, y, z = Cartesian coordinates
E = Young's modulus
$\underline{E}, \underline{E}_B, \underline{E}_U$ = propagation modes
L = length of pipe
MMB = coherent multimode fiber bundle
M_T = applied torque
NA = numerical aperture
P = applied load
SMB = coherent monomode fiber bundle
U_θ = tangential component of displacement
V = dimensionless waveguide parameter
W = displacement component along the line of sight
β_j = propagation constant
Δ = core to cladding index difference
θ_c = critical angle
λ = wavelength
ν = Poisson's ratio
ϱ = radius of fiber core
$\phi(Z)$ = angle of twist
ω = angular velocity
ℓ = length of fiber

J.A. Gilbert (SESA Member) is Associate Professor, Department of Civil Engineering, University of Wisconsin-Milwaukee, Milwaukee, WI 53201. T.D. Dudderar (SESA Member) is Member, Technical Staff, Bell Laboratories, Murray Hill, NJ 07974. M.E. Schultz and A.J. Boehnlein are Research Assistants, Department of Civil Engineering, University of Wisconsin-Milwaukee, Milwaukee, WI 53201.

Paper was presented at 1982 SESA Spring Meeting held in Oahu and Maui, HI on May 24-28, 1982.

Original manuscript submitted: October 26, 1981. Authors notified of acceptance: June 15, 1982. Final version received: August 15, 1982.

Introduction

There has been a great explosion in fiber-optic technology in recent years because of the growing interest in the application of fiber optics to communication systems.[1] Research on optical fibers has now progressed to the point where low-loss fibers suitable for practical non-communications applications have become readily available; however it is essential to evaluate which types of fibers are best suited for which purpose and to design appropriate optimized systems. This paper deals with fundamental advantages of and problems associated with the application of a monomode optical fiber to holographic interferometry.

Fiber Optics

Light can be forced to travel through a thin-glass fiber whose cross section and optical properties are designed based on the phenomenon of total internal reflection. Two of the most common fibers commercially available are graded index and step index. The graded-index fiber is produced so that the index of refraction decreases as the distance from the axis of the fiber increases, while a step-index fiber consists of a core, with refractive index n_{co}, surrounded by a cladding of lower refractive index, n_{cl}. In a step-index fiber, light traveling through the core is reflected back from the cladding provided that the angle of incidence is less than the critical angle, θ_c, defined by

$$\theta_c = \cos^{-1}(n_{cl}/n_{co}) \tag{1}$$

Step-index fibers are used in this investigation.

The numerical aperture (NA), or acceptance angle, of a step-index fiber is given by

$$NA = n_{co}(2\Delta)^{1/2} \tag{2}$$

where Δ is the relative index difference between the core and the cladding defined by

$$\Delta = \frac{n_{co}^2 - n_{cl}^2}{2n_{co}^2} \tag{3}$$

Step-index fibers which have a large numerical aperture, or acceptance angle. are classified as multimode. In addition to rays or modes traveling straight through the fiber, some trace coarse zigzag paths down the guide. The electric field along the fiber can be written in terms of the modes of the system as[2-5]

$$\underline{E} = \underline{E}_B + \underline{E}_U \tag{4}$$

where $\underline{E}_B$ represents a finite number of bound modes which in an ideal, nonabsorbing fiber propagate with no change or attenuation, while $\underline{E}_U$ represents an integral that includes all energy which, even for an ideal fiber, leaves the core and radiates into the cladding.

For light of angular frequency ω, propagating through the fiber in the z direction,

$$\underline{E}_B = \sum_{j=1}^{N} a_j \underline{e}_j(x,y,\beta_j) e^{i(\omega t - \beta_j z)} \tag{5}$$

where a_j, $\underline{e}_j$ and β_j are the modal amplitude, modal field and propagation constant for mode j, respectively. The modal amplitude is determined by the source exciting the fiber while the modal-propagation constants are a function of the dimensionless waveguide parameter, V. The latter can be defined in terms of the indices of refraction, the fiber-core radius, ϱ, and the light wavelength, λ, as,

$$V = \left(\frac{2\pi\varrho n_{co}}{\lambda}\right)\left(1 - \frac{n_{cl}^2}{n_{co}^2}\right)^{1/2} \tag{6}$$

Generally speaking, the modes propagating in an optical fiber can be uniquely and completely defined through the two parameters ϱ and V. The number, N, of bound modes which propagate in a step-index fiber depends monotonically on V; and, when V is large, $N \simeq \frac{1}{2} V^2$. For example, hundreds of modes propagate along fibers with $V > 20$. Each mode propagates with a different group velocity and modal dispersion occurs along the fiber.[6] Although spatial coherence is practically preserved in each wavefront transmitted through the fiber, detrimental modal interaction can be extremely severe when the fiber is applied to holographic interferometry.[7,8]

Intermodal dispersion decreases when the dimensionless waveguide parameter, V, becomes small, and a step-index fiber is classified as monomode when $V < 2.405$. In this case, only one mode propagates through the fiber and intermodal dispersion is minimized.[9]

For a given wavelength, eq (6) shows that V can be decreased by minimizing the difference in refractive indices of the core and cladding and/or decreasing the fiber diameter. A small fiber diameter increases difficulty in launching and joining; therefore, a practical step-index, monomode fiber can be manufactured most simply by combining materials with very similar refractive indices. Fibers of this type are called weakly guiding[10] and the relative index difference, Δ, defined by eq (3), becomes

$$\Delta = \frac{n_{co} - n_{cl}}{n_{co}} \tag{7}$$

as $n_{cl} \rightarrow n_{co}$. There are practical limitations which define the lower bound for the latter; 0.05 percent to 0.15 percent are typical values for Δ. For visible laser light, eq (6) predicts a required core diameter of a few microns. This places stringent demands on fiber technology.

A considerable amount of effort has gone into developing various descriptions of the propagation phenomena in monomode fibers and examining the relative merits and accuracies of the different material candidates for their composition. Recently, Bell Laboratories manufactured a step-index, monomode fiber of core radius $\varrho = 7.3\ \mu$ with the following characteristics at $\lambda = 633$ nm,

$$\begin{aligned} NA &= 0.1159 \\ n_{co} &= 1.4631 \\ n_{cl} &= 1.4585 \end{aligned} \tag{8}$$

In this investigation, the exit end of this monomode fiber is used as the source of illumination for generating a hologram. The far-field radiation can be calculated using the Fraunhofer formula, as the fiber-end aperture is very small compared with the distance to the test surface.[11]

The intensity distribution originating from a well prepared fiber end is nearly gaussian in shape[12-14] and is similar to the gaussian spherical wave produced by a spatial filter in a conventional holographic arrangement.[11] The central portion of the cone of radiation provides a reasonably uniform illumination of the test surface; however, the small numerical aperture of the fiber limits the divergence of the emanating wavefront. Consequently, a monomode fiber acts like a spatial filter equipped with a low-powered microscope objective. Micro lenses can be used to collimate the beam or to produce additional beam divergence.

Fiber Bundles

Individual fibers cannot transmit images; therefore, several thousand fibers must be collected into a bundle to convey image amplitude and phase information from the test surface to the photographic plate in cases where optical access to the test surface is limited. A real image, focused on the entrance end of the bundle, can be transmitted provided that the relative orientation of each fiber in the bundle is maintained throughout its length. The bundle is classified as coherent. Each fiber transmits a different amount of light and the image at the exit end is composed of discrete components of varying intensity. Since the MMB is a light guide as opposed to a lens, a three-dimensional object must be within the depth of field of the system used to project its image onto the entrance end. The real image on the exit end can be focused on the photographic plate and superimposed with a reference wavefront to generate an image-plane hologram. The apparent proximity of the object to the plate decreases the coherence requirement on the source during reconstruction which allows a real image to be viewed in white light.[15,16]

Although it would be desirable to use a monomode bundle for this study, all of the coherent bundles now available are composed of multimode fibers. Each fiber has a large core surrounded by a thin cladding, which makes for a very efficient MMB, since the efficiency of a fiber bundle is measured in terms of the percentage of useable transmission area and the amount of light which passes through it. On the other hand, the commercial monomode fiber used in these experiments, characterized by eq (8), has a small core and a thick cladding (about 1:12) which would make a very inefficient bundle.

Present efforts are being directed towards developing a preform using compatible glasses of similar refractive indices which, when drawn, will result in a monomode

fiber of larger core to cladding ratio to be incorporated into a highly efficient, coherent, single-mode fiber bundle or SMB.

Holographic Applications of Fiber Optics

Light emitted from the exit end of an optical fiber was used in holography as the reference wave in recording a hologram and/or the illuminating wave in reconstructing it.[17,18] Individual fibers were also used in the object beam to illuminate the test surface. Although the problems associated with such an application have been investigated,[19,11] object wavefronts recorded on the hologram were not captured through fiber optics and direct optical access to the test surface was required. Recently, a coherent bundle was inserted between the object and the photographic plate to convey phase information to the hologram for subsequent displacement analysis in cases where optical access was limited.[7] These concepts were extended[8] and displacement was measured over the full-field using coherent bundles made up from individual multimode fibers with step-index profiles or MMBs. In these deformation studies, fiber optics were used to gain access to remote areas of a structure, to reduce the number of optical components necessary for testing and to increase the flexibility of the experimental setup. Multimode fibers, however, transmit many modes, or wavefronts, which can interact during or between exposures, resulting in poor holographic recordings.

Flexible monomode fibers have not been used for holographic work due to their commercial nonavailability; however, one investigator reported launching a fundamental HE_{11} mode through a fiber designed for single-mode operation at 900 nm by careful excitation of the fiber.[11] Results indicated that the reduction in modal interaction eased environmental requirements for holography.

The present study used a step-index, monomode fiber designed and manufactured at Bell Laboratories for communication purposes at 633 nm. This fiber actually transmits two orthogonal polarizations of the fundamental mode which, because of noncircularity of the core or stress-induced birefringence, have slightly different propagation constants,[20-22] so there is some modal dispersion but this is a very small effect, especially in comparison with a commercial multimode fiber. A single loop can also be introduced in the fiber to suppress one of these modes. It would be expected that by minimizing intermodal dispersion, holograms can be recorded with better diffraction efficiency and stringent requirements for vibration isolation ordinarily associated with holographic testing can be somewhat relaxed.

In holographic interferometry, two reconstructed hologram images corresponding to the undeformed and deformed test surface are superimposed. A displacement fringe pattern is observed which is governed by[23]

$$(\hat{\underline{e}}_1 - \hat{\underline{e}}_2) \cdot \underline{d} = n\lambda \qquad (9)$$

where $\underline{d}$ is the displacement vector, n the fringe order number, λ the wavelength, and $\underline{e}_1$ and $\underline{e}_2$ are unit vectors along the directions of propagation from the source and to the observation point respectively, drawn to/from the point under consideration. In short, the observed displacement fringes are due to the change in optical-path length which occurs between exposures. These path-length changes give rise to a distribution of phase differences between the reconstructed wavefronts which results in areas of constructive or destructive interference and are seen as light and dark fringes. The component of displacement measured at each point depends upon the location of the source and on the point of observation.

The exit end of the monomode fiber which illuminates the test object acts as the source point, while the entrance end of the coherent multimode fiber bundle is at the point of observation. The assembly of rays inherent in each fiber in the imaging bundle may be described in terms of a mean path length. This is defined as the average of the path lengths for all rays weighted by their respective transmittances; respective path lengths distribute around this mean value.[24] The minimum and maximum optical-path length in a step-index, multimode fiber of length ℓ are $n_{co}\ell$ for the ray traveling straight down the core and $(n_{co}^2/n_{cl})\ell$ for a ray at the critical angle, respectively. The spread of the distribution $\Delta\ell$, however, does not exceed $\Delta\ell_{max} = n_{co}(n_{co}/n_{cl} - 1)\ell$.

When the undeformed and deformed states of the object surface are transmitted through the coherent bundle, all of the modes experience equal changes in optical-path length for each object point focused on the entrance end. In general, however, many object points are focused on a single fiber and several phase differences are transmitted. Upon superposition, the intensity in each fiber is pro-

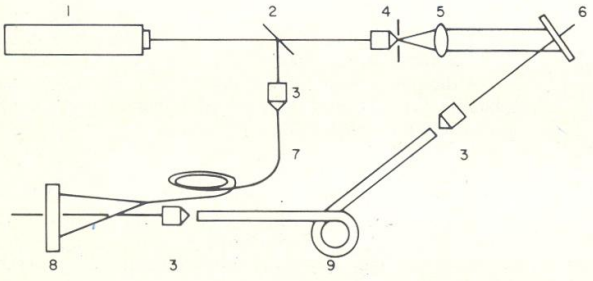

1. C.W. LASER; 2. BEAM SPLITTER; 3. MICROSCOPE OBJECTIVES;
4. BEAM EXPANDER & SPATIAL FILTER; 5. COLLIMATING LENS;
6. PHOTOGRAPHIC PLATE(HOLOGRAM); 7. SINGLEMODE OPTICAL FIBER;
8. TEST OBJECT; 9. COHERENT MULTIMODE OPTICAL FIBER BUNDLE.

Fig. 1—The experimental setup

portional to the mean displacement over the core and the overall image includes a fringe pattern governed by eq (9).

Experiments

Experiments were initially carried out to demonstrate the feasibility of using the monomode fiber characterized by eq (8) to illuminate two- and three-dimensional test surfaces for holographic deformation analysis. Additional tests, some of which were carried out using an individual multimode fiber for comparison purposes, showed the monomode fiber to be clearly superior for holographic recording, primarily because vibration-isolation requirements became less stringent. In all tests, real images of the test surfaces were transmitted to the hologram through a 2-mm diameter, MMB capable of resolving 27 line pairs/mm and composed of individual 12-μ diameter fibers.

As shown in Fig. 1, the monomode fiber was situated with its exit end parallel to the entrance end of the MMB. A reference wavefront recorded the phase changes which occurred between exposures. The surface of a clamped centrally loaded circular disk of 7.62-cm diameter was positioned normal to the fiber optics at a sufficiently large distance so that the displacement-phase relation governed by eq (9) reduces to

$$W = \frac{n\lambda}{2} \tag{10}$$

where λ is the wavelength, n the fringe order number and W is the displacement component measured along the line of sight.

A He-Ne laser, $\lambda = 633$ nm, was used to record a hologram of the undeformed disk on a photographic plate. The center of the disk was displaced under load 3.81×10^{-3} cm along the line of sight and a hologram of the deformed surface was recorded, superimposed on the initial hologram. Figure 2 shows the white-light reconstruction of the processed double-exposure hologram with the resulting fringe pattern corresponding to displacement measured normal to the plane of the clamped disk. The jagged appearance of the displacement fringes can be attributed to the manner in which the individual fibers in the MMB convey phase information and to the density and construction of the MMB itself.[8] The deflection of the disk at a distance r from the center is given by[25]

$$W = \frac{Pr^2}{8\pi D} \log \frac{r}{a} + \frac{P}{16\pi D}(a^2 - r^2) \tag{11}$$

where

$$D = \frac{Eh^3}{12(1 - \nu^2)} \tag{12}$$

Equations (11) and (12) are for a disk of radius a and thickness h with Young's modulus and Poisson's ratio of E and ν, respectively. The load, P, was determined from the change in deflection of the center of the disk imposed between exposures. Figure 3 shows a computer generated plot of the fringe loci predicted for our experiment in which

$$\begin{aligned} a &= 3.81 \text{ cm} & E &= 27.58 \times 10^5 \text{ kPa} \\ h &= 0.318 \text{ cm} & \nu &= 0.35 \end{aligned} \tag{13}$$

Light, integer fringes in Fig. 2 agree well with the theoretical fringe loci.

A similar test involving a three-dimensional subject was conducted using a cylindrical pipe of length L. The pipe was rigidly fixed at end $Z/L = 0$ and a torque was applied at $Z/L = 1$, to produce a state of pure torsion. Z is measured along the longitudinal axis of the pipe from

Fig. 2—Displacement pattern of a centrally loaded clamped circular disk using an individual monomode fiber for illumination and a multimode coherent bundle of 12-μ diameter fibers for image transmission

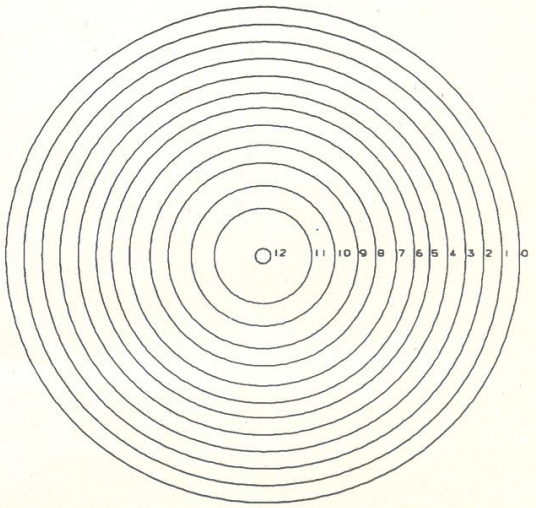

Fig. 3—Computer-generated plot of theoretical fringe loci for the centrally loaded clamped circular disk

the fixed support towards the end at which the torque, M_T, is applied. The surface of the pipe was within the depth of field of the lens system used to project its image on the entrance end of the coherent bundle. This ensured that all points of the image projected on the photographic plate were in focus. Figure 4 shows the fringe pattern measured along the line of sight, that is perpendicular to the plane of the figure in the region $0 \leq Z/L \leq \frac{1}{3}$.

The tangential component of displacement is given by[26]

$$U_\theta = \frac{d_0}{2}\,\phi(Z) \tag{14}$$

where d_0 is the outer diameter of the pipe and $\phi(Z)$ is the angle of twist. The latter is given by

$$\phi(Z) = \frac{64 M_T(1+\nu)Z}{\pi[d_0^4 - d_i^4]E} \tag{15}$$

In eq (15), d_i is the inner diameter of the pipe, ν the Poisson's ratio, and E is the Young's modulus.

The displacement along the line of sight is

$$W = U_\theta \cos\theta = \frac{d_0}{2}\,\phi(Z)\cos\theta \tag{16}$$

where θ is the radial coordinate. Figure 5 shows the theoretical fringe loci in the region $0 \leq Z/L \leq \frac{1}{3}$: 0 deg $< \theta <$ 180 deg, for this experiment in which

$$\begin{array}{ll} M_T = 0.38 \text{ Nm} & E = 27.58 \times 10^5 \text{ kPa} \\ d_0 = 4.85 \text{ cm} & \nu = 0.37 \\ d_i = 4.06 \text{ cm} & L = 17.78 \text{ cm} \end{array} \tag{17}$$

The fringe patterns in Figs. 4 and 5 agree well with each other at points removed from the fixed constraint. Careful examination of the pattern shown in Fig. 4 reveals some fringes on the support frame, indicating that deformation and/or rigid-body motion occurred in this region. If effectively rigid, the entire support would be completely free of fringes.

The two tests described above were repeated using an individual multimode fiber to illuminate the test surfaces for comparison purposes. Reconstructions were of comparable quality to those shown in Figs. 2 and 4, provided that the fiber remained stationary during and/or between exposures.

Additional stability tests were performed using the monomode and then the multimode fiber for illumination. In these tests, the illuminating fiber was modulated during and between exposures using air currents from a small fan. Only the ends of each fiber were constrained. There was no noticeable effect on the holographic recordings for the monomode fiber; however, no reconstructions were obtained when the modulated multimode fiber was used for illumination. We therefore conclude that monomode fibers are clearly superior for holographic recording, primarily because vibration-isolation requirements become less stringent with the decrease in modal interaction.

Discussion and Conclusion

Holographic deformation fringes on the centrally loaded clamped circular disk and at points removed from the fixed support on the torsion specimen agreed well with theory. Unexpected deformation and/or rigid-body motion at the fixed end of the torsion specimen was revealed by the presence of fringes on the supporting structure. In general, fringe patterns obtained on these flat and curved surfaces are of better quality than those previously obtained using multimode fiber bundles to illuminate the object[7,8] and diffraction efficiency is not affected by modulations in the illuminating fiber during and/or between exposures. Further improvements in fringe quality will be made when the monomode fiber bundle becomes available.

The basic characteristics of radiation relevant to holography are coherence, the form of the wavefronts and polarization. Wavefronts of laser light maintain their coherence properties even after extreme distortions by random media; consequently, for the most part coherence is preserved in the wavefronts transmitted through fiber optics and both multimode and monomode fibers can be used as coherent light guides for holography. It has been shown, however, that a holographic reconstruction becomes brightest when the object and reference wavefronts are linearly polarized perpendicular to the plane containing their axes of propagation.[27] The polarization in the multimode coherent bundle used for this investi-

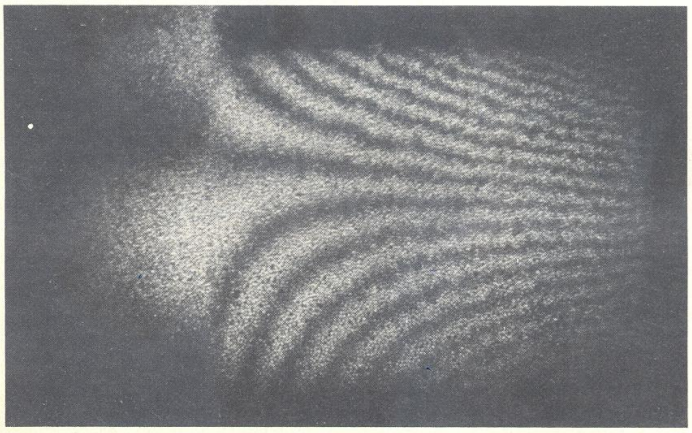

Fig. 4—Displacement pattern of a pipe subjected to pure torsion using an individual monomode fiber for illumination and a multimode coherent bundle of 12-μ diameter fibers for image transmission

gation is distributed at random throughout the radiation pattern due to scattering within the fibers and to the fact that each guided mode has its own polarization state. The polarization of coherent light passing through monomode fibers can be controlled to some degree and has been studied by several investigators.[21,28,29] The sole guided mode really corresponds to two modes having the same configuration but with orthogonal polarizations.[5] Coupling often occurs between these modes and light becomes elliptically polarized. Linearly polarized light can be obtained by modifying the fiber profile, for example, using an elliptical core,[27] or more readily by bending the fiber into a specified radius. The latter can be accomplished with very little effort and very little penalty. This may, however, induce mechanical stress which could affect other transmission characteristics of the fiber.[30] These would have to be taken into consideration if the configuration of the bend were modified during or between exposures.

Initial feasibility studies carried out with the setup shown in Fig. 1 have shown that vibration isolation is not required at the test site provided that the laser, launching optics and photographic plate are isolated on a vibration-free table. A monomode fiber bundle further increases optical stability by decreasing modal interaction and allows displacement to be measured in remote areas of a structure, potentially at locations removed from the laboratory. In some cases, this may require a second monomode fiber in the reference beam to keep the object and reference path lengths within the coherence length of the laser, but really represents no problem.

In conclusion, monomode fibers are well suited for holographic deformation studies and will serve as valuable new tools for the experimental stress analyst.

Acknowledgment

Research was supported by the Army Research Office (Grant No. DAAG-29-80-K-0028) and Bell Laboratories. Special thanks are extended to R.D. MacDougall and K.F. Leeb of American Cystoscope Makers, Inc., for their cooperation and interest in the project and to J.H. Bennewitz for his help in preparing the figures for the paper.

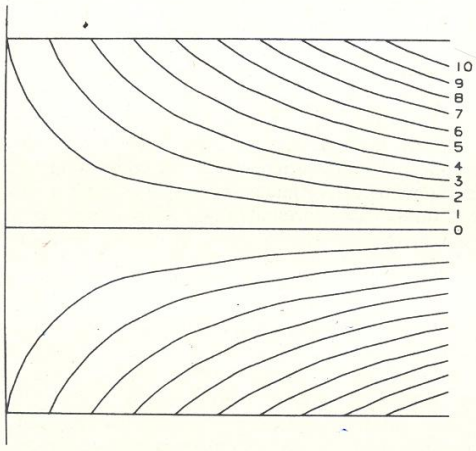

Fig. 5—Computer-generated plot of theoretical fringe loci for the pipe subjected to pure torsion

References

1. Miller, S.E. and Chynoweth, A.G., editors, *Optical Fiber Telecommunications, Academic Press, New York, San Francisco, London (1979).*

2. Collin, R.E., *Field Theory of Guided Waves, McGraw-Hill, New York (1960).*

3. Kapany, N.S. and Burke, J.J., *Optical Waveguides, Academic Press, New York (1972).*

4. Marcuse, D., *Light Transmission Optics, Van Nostrand, New York (1972).*

5. Marcuse, D., *Theory of Dielectric Optical Waveguides, Academic Press, New York (1974).*

6. Pask, C., Snyder, A.W. and Mitchell, D.J., *"Number of Modes on Optical Waveguides," J. Opt. Soc. Amer.,* **65** *(15), 356-357 (March 1975).*

7. Gilbert, J.A. and Herrick, J.W., *"Holographic Displacement Analysis with Multimode Fiber Optics,"* EXPERIMENTAL MECHANICS, **21** *(8), 315-320 (Aug. 1981).*

8. Gilbert, J.A., Schultz, M.E. and Boehnlein, A.J., *"Remote Displacement Analysis Using Multimode Fiber Optic Bundles," Proc. SESA Spring Meeting, Dearborn, MI, 41-43 (May 1981).*

9. Marcuse, D., *"Loss Analysis of Single-Mode Fiber Splices," Bell Syst. Tech. J.,* **56** *(5), 703-718 (May 1977).*

10. Gloge, D., *"Weakly Guiding Fibers," Appl. Opt.,* **10** *(10), 2252-2258 (Oct. 1971).*

11. Leite, A.M.P.P., *"Optical Fibre Illuminators for Holography," Opt. Comm.,* **28** *(3), 303-308 (March 1979).*

12. Peterman, K., *"Fundamental Mode Micro Bending Loss in Graded Index and W Fibers," Opt. Quantum Electron.,* **9** *(2), 167-175 (Feb. 1977).*

13. Gambling, W.A. and Matsumura, H., *"Propagation in Radially Inhomogeneous Single-Mode Fibers," Opt. Quantum Electron.,* **10** *(1), 31-40 (Jan. 1978).*

14. Marcuse, D., *"Gaussain Approximation of the Fundamental Modes of Graded Index Fibers," J. Opt. Soc. Amer.,* **68** *(1), 103-109 (Jan. 1978).*

15. Sciammarella, C.A. and Chawla, S.K., *"A Lens Holographic-moiré Technique to Obtain Components of Displacement and Derivatives,"* EXPERIMENTAL MECHANICS, **18** *(10), 373-381 (Oct. 1978).*

16. Gilbert, J.A. and Exner, G.A., *"Holographic Displacement Analysis Using Image-plane Techniques,"* EXPERIMENTAL MECHANICS, **18** *(10), 382-388 (Oct. 1978).*

17. Suhara, T., Nishihara, H. and Koyama, J., *"The Far Field Patterns of the Light Emitted from a Fiber and Their Application to Holography," Proc. Annual Meeting of IECE of Japan, S15-2 (in Japanese) (March 1975).*

18. Suhara, T., Nishihara, H. and Koyama, J., *"Analysis of the Radiation Characteristics of Optical Fibers for the Hologram Reconstruction," Report of Fukusha - Kagaku Kenkyukai (in Japanese) (Dec. 1974).*

19. Suhara, T., Nishihara, H. and Koyama, J., *"Far Radiation Field Emitted from an Optical Fiber and Its Application to Holography," Trans. of the IECE of Japan,* **E60** *(10), 533-540 (Oct. 1977).*

20. Rashleigh, S.C. and Ulrich, R., *"Polarization Mode Dispersion in Single-mode Fibers," Opt. Let.,* **3** *(2), 60-62 (Aug. 1978).*

21. Ramaswamy, V., Standley, R.D., Sze, D. and French, W.G., *"Polarization Effects in Short Length, Single-mode Fibers," Bell Syst. Tech. J.,* **57** *(3), 635-651 (March 1978).*

22. Ramaswamy, V. and French, W.G., *"Influence of Non-circular Core on Polarization Performance of Single Mode Fibers," Elect. Let.,* **14** *(5), 143-144 (March 1978).*

23. Sollid, J.E., *"Holographic Interferometry Applied to Measurements of Small Static Displacements of Diffusely Reflecting Surfaces," Appl. Opt.,* **8** *(8), 1587-1595 (Aug. 1969).*

24. Suzuki, T., *"Interferometric Uses of Optical Fiber," Japanese J. of Appl. Phys.,* **5** *(11), 1065-1074 (Nov. 1966).*

25. Timoshenko, S. and Woinowsky-Krieger, S., *Theory of Plates and Shells, McGraw-Hill, New York (1959).*

26. Timoshenko, S., *Strength of Materials, D. Van Nostrand Co., New York (1940).*

27. Rose, H.W., Williamson, T.L. and Collins, Jr., S.A., *"Polarization Effects in Holography," Appl. Opt.,* **9** *(10), 2394-2396 (Oct. 1970).*

28. Simon, A. and Ulrich, R., *"Evolution of Polarization Along a Single-mode Fiber," Appl. Phys. Let.,* **31** *(8), 516-520 (Oct. 1977).*

29. Stolen, R.H., Ramaswamy, V., Kaiser, P. and Pleibel, W., *"Linear Polarization in Birefringent Single-mode Fibers," Appl. Phys. Let.,* **33** *(8), 699-701 (Oct. 1978).*

30. Namihira, Y., Kudo, M. and Mushiake, Y., *"Effect of Mechanical Stress on the Transmission Characteristics of Optical Fiber," Electronics and Comm. in Japan,* **60-C** *(7), 107-115 (July 1977).*